Published in final edited form as:
Hear Res. 2011 July ; 277(1-2): 204–210. doi:10.1016/j.heares.2010.12.021.

Effects of Vestibular Prosthesis Electrode Implantation and Stimulation on Hearing in Rhesus Monkeys

Chenkai Dai, MD, PhD, **Gene Y. Fridman, PhD**, and **Charles C. Della Santina, PhD, MD**[*]
Departments of Otolaryngology – Head & Neck Surgery and Biomedical Engineering Johns Hopkins University School of Medicine, Baltimore

Abstract

To investigate the effects of vestibular prosthesis electrode implantation and activation on hearing in rhesus monkeys, we measured auditory brainstem responses (ABR) and distortion product otoacoustic emissions (DPOAE) in four rhesus monkeys before and after unilateral implantation of vestibular prosthesis electrodes in each of 3 left semicircular canals (SCC). Each of the 3 left SCCs were implanted with electrodes via a transmastoid approach. Right ears, which served as controls, were not surgically manipulated. Hearing tests were conducted before implantation (BI) and then 4 weeks post implantation both without electrical stimulation (NS) and with electrical stimulation (S). During the latter condition, prosthetic electrical stimuli encoding 3 dimensions of head angular velocity were delivered to the 3 ampullary branches of the left vestibular nerve via each of 3 electrode pairs of a multichannel vestibular prosthesis. Electrical stimuli comprised charge-balanced biphasic pulses at a baseline rate of 94 pulses/sec, with pulse frequency modulated from 48–222 pulses/s by head angular velocity. ABR hearing thresholds to clicks and tone pips at 1, 2, and 4 kHz increased by 5–10 dB from BI to NS and increased another ~5 dB from NS to S in implanted ears. No significant change was seen in right ears. DPOAE amplitudes decreased by 2–14 dB from BI to NS in implanted ears. There was a slight but insignificant decrease of DPOAE amplitude and a corresponding increase of DPOAE/Noise floor ratio between NS and S in implanted ears.

Vestibular prosthesis electrode implantation and activation have small but measurable effects on hearing in rhesus monkeys. Coupled with the clinical observation that patients with cochlear implants only rarely exhibit signs of vestibular injury or spurious vestibular nerve stimulation, these results suggest that although implantation and activation of multichannel vestibular prosthesis electrodes in human will carry a risk of hearing loss, that loss is not likely to be severe.

Keywords

multichannel; vestibular prosthesis; electrode; implantation; electrical stimulation; hearing; labyrinth; vestibular; vestibular implant

[*]Corresponding author: Charles C. Della Santina, PhD MD (last name = “Della Santina”), Vestibular NeuroEngineering Laboratory (same address/affiliation for all authors), Johns Hopkins School of Medicine, 720 Rutland Ave., Ross Bldg Rm 830, Baltimore, MD 21205 USA, (410) 502-7909 (voice), (410) 614-2439 (fax), charley.dellasantina@jhu.edu.

DISCLOSURE STATEMENT

All authors have participated in experiment design, data acquisition, analysis, and manuscript preparation, and all have approved the final article. Disclosure of potential conflicts of interest: CD-none; GYF-patent application pending; CCDS- patent application pending, equity interest in Labyrinth Devices LLC.

1 INTRODUCTION

The vestibular labyrinth provides the dominant sensory input regarding head movement and orientation. Damage to the labyrinth can result in acute vertigo followed by chronic oscillopsia and disequilibrium that interfere with locomotion, driving and other activities of daily life. Apart from rehabilitation exercises and cessation of vestibular suppressant medications, there is no effective treatment for profound bilateral loss of labyrinthine function.

Della Santina *et al.* (2007) developed a multichannel vestibular prosthesis that simultaneously encodes head rotations in all 3 dimensions, resolves them into canal-plane components, and presents them as pulse-frequency-encoded stimuli to the ampullary nerves innervating each of 3 semicircular canals (SCCs). Restoring function with the vestibular prosthesis requires electrode implantation into 3 SCCs and delivery of electrical stimuli via those electrodes to the ampullary nerve branches. Since the auditory and vestibular portions of the inner ear and eighth cranial nerve are intimately connected, a prosthesis meant to evoke vestibular nerve activity might inadvertently affect the cochlea or the cochlear nerve. Thus, two questions arise: (1) Does vestibular prosthesis electrode implantation affect cochlear function? (2) Does electrical stimulation intended for the vestibular nerve interfere with hearing?

Potential hearing risks of electrode implantation alone include conductive hearing loss (e.g., ossicular disruption) and sensorineural hearing loss (e.g., caused by damage to the membranous labyrinth or cochlear nerve) (Gacek & Gacek, 2002; Epley, 1980). Even if implantation preserves all auditory structures, stimulus currents from a vestibular prosthesis might activate sufficient cochlear nerve fibers to cause tinnitus, activate acoustic reflexes that alter middle ear mechanics, or otherwise interfere with normal hearing.

Experiments in animal models support the feasibility of a vestibular prosthesis (Gong and Merfeld, 2000, 2002; Della Santina *et al.*, 2007; Fridman *et al.* 2010; Davidovics *et al.*, 2010; Chiang *et al.*, 2010; Della Santina *et al.*, 2010), but clinical trials should not proceed before clarifying the risks of vestibular prosthesis implantation and stimulation on hearing. One previous study in chinchillas (Tang *et al.*, 2009) showed that SCC electrode implantation caused hearing loss in 2 of 6 implanted ears as compared to sham surgery control ears. Those results suggest a need to evaluate the effect of electrode implantation on hearing in rhesus monkeys, whose anatomy is more similar to that of humans. The larger size and structural differences between the inner ears of simian primates and chinchillas offer hope that deleterious effects of vestibular electrode implantation observed in chinchillas hearing may not translate to monkeys or to humans. Moreover, the advent of new electrode array designs allowing more precise and less traumatic electrode implantation (Chiang *et al.*, 2010) may reduce the risk of cochlear injury and inadvertent spread of prosthetic current to the cochlear nerve.

We hypothesized that the hearing loss induced by electrode implantation in rhesus monkeys would be less frequent and less severe than that reported for chinchillas. To test this hypothesis and to evaluate the possible effects of vestibular prosthesis stimuli on hearing, we measured hearing using ABR and DPOAE in four rhesus monkeys before and after implantation and with prosthetic stimulation either on or off.

2 METHODS

2.1 Subjects and experiment paradigm

Four rhesus monkeys (female, 3–6 kg) without history of risk factors for hearing loss (prior ototoxic drugs, radiation, acoustic trauma, ear disease) were used in this study. ABR and DPOAE responses were measured on both ears of the four monkeys before surgery and four weeks after vestibular prosthesis electrode implantation, both during and without electrical stimulation via the implanted electrodes. All procedures used in this study were in accordance with a protocol approved by the Animal Care and Use Committee of the Johns Hopkins University School of Medicine and consistent with European Community Directive 86/609/EEC.

2.2 Auditory brainstem response

The ABR recording technique is similar to that we have previously described (Tang *et al.*, 2009); except that ABRs were acquired using a clinical grade auditory evoked potential system (Nicolet Spirit) with sampling rate 100 kHz. ABR measurements were recorded with solid gel skin electrodes (GN Otometrics) attached in the midline above the supraorbital ridge, on the right and left ear lobes, and on the cheek ipsilateral to the test ear (ground). Individual electrode impedances were below 3 kΩ. Before any measurements, a sound level meter and microphone (Nicolet) were used to calibrate the ABR speakers in the experimental set-up without the monkey. Monkeys were anesthetized with ketamine (5–10 mg/kg IM) during ABR measurements. Monkeys sat on a chair inside a sound-isolating room, where they were exposed to clicks and tone pips at 1, 2, and 4 kHz emitted from a free field speaker facing the test ear while the other ear was occluded with a foam earplug. The average ABR waveform was based on 200 presentations of the stimulus given at a rate of 30 per second. At each frequency, the level of the stimulus was presented in 10 dBSPL descending increments until the ABR waveform was no longer visible above the noise floor, then in alternating 5 dBSPL ascending and descending increments until a clear threshold was identified.

2.3 Distortion product otoacoustic emissions

Distortion product otoacoustic emissions (DPOAEs) were measured using a clinical grade system (Biologic, Model 580-NAVPR2), two Etymotic ER-2 earphones, a probe unit containing an Etymotic ER-10B microphone, and an Etymotic amplifier providing 40 dB of amplification. Silicone tubing (0.95 mm OD, 0.5 mm ID) transmitted the sound generated by the two earphones through the probe housing and into the ear canal. Microphones were recalibrated before each DPOAE measurement.

The cochlea was stimulated with two primary frequencies (f1 and f2, where f2>f1), and the distortion product (2f1 – f2) emitted by the cochlea was measured. These emissions were measured using an f2/f1 ratio = 1.22 while f2 was varied from 1, 2, 3 and 4 kHz. Tone levels of primary frequencies (L1 and L2) were constant at 65 and 55 dB SPL, respectively. Absolute DPOAE level and noise floor level were measured, and DPOAE/noise floor ratio (DP/NF ratio) was determined by subtracting the noise floor from the DPOAE level in dB. Both absolute DPOAE level and DPOAE/noise ratios at 1, 2, 3 and 4 kHz were measured as an assessment of cochlear function.

2.4 Electrode Array

Electrode arrays designed and fabricated for the present study are much more like those of cochlear implants in clinical use than were the electrodes used for study of chinchillas (Tang *et al.*, 2009). Based on species-specific measurements from 3D reconstructions of micro-computed tomography images of existing temporal bone specimens for normal rhesus

macaque monkeys, each electrode array comprises 9 active and 2 reference electrodes, with active electrodes partly embedded within a silicone carrier designed to self-orient within the ampullae during implantation through small ampullotomies made near the junction of each SCC thin segment and ampulla. All electrode pads and leads are 90/10 Platinum/Iridium. Details of the electrode array design have been presented in detail elsewhere (Chiang *et al.* 2010).

2.5 Surgical implantation of intralabyrinthine electrodes

Surgical procedures including head cap placement, scleral coil implantation and electrode implantation have been described in detail elsewhere (Minor *et al.* 1999; Lasker *et al.* 2000; Chiang *et al.* 2010). All surgery was performed under sterile conditions and general inhalational anesthesia (sevoflurane 3–5%) supplemented by local anesthesia (field block with lidocaine 1% with 1:100K epinephrine).

Head cap placement began with exposure of the calvarium, placement of approximately 12 self-tapping titanium bone screws, and formation of a poly-methyl methacrylate mound engulfing the screws and conforming to the exposed calvarium. A cylinder chamber (diameter of 6 cm) was mounted atop the mound at an orientation such that the animal's horizontal stereotaxic plane could later be made Earth-horizontal when affixed to a head-restraining apparatus during subsequent testing (Minor *et al.*, 1999).

Dual scleral coil implantation for subsequent 3D eye movement measurements using the search coil technique was performed as previously described (Minor and Goldberg 1991; Paige and Tomko 1991; Straumann *et al.*, 1995; Migliaccio *et al.*, 2004). A prefabricated search coil (diameter 14.5 mm, Teflon-coated, braided stainless steel wire, Cooner Wire AS631, Chatsworth CA) was implanted in the frontal plane about the limbus of left eye as a directional coil. A second coil with diameter ~12 mm was implanted about the superior rectus insertion as a torsional coil. Leads were run within subperiosteal tunnels to the inside of the head cap chamber.

Electrode implantation began with a left cortical mastoidectomy followed by exposure of the horizontal, posterior, and superior SCCs, each of which was then was opened via a fenestration (diameter ~0.5 mm) near the junction of the thin segment and ampulla. The tip of each electrode array was inserted to rest near the crista termination of the corresponding ampullary nerve. Each ampullotomy was gently packed with fascia, and the postauricular incision was closed.

2.6 Eye movement recording during prosthetic stimulation

We recorded eye movement responses to prosthetic electrical stimulation in darkness using a 3D eye coil system and signal processing methods described in detail previously (Straumann *et al.*, 1995; Migliaccio *et al.*, 2004). In brief, an alert animal was seated in a plastic chair enclosure with its head restrained by a head cap. The animal was otherwise free to move within the enclosure. A Johns Hopkins MVP2 multichannel vestibular prosthesis was affixed to the head cap so that its three head angular velocity sensors were aligned with the corresponding mean SCC planes (Blanks *et al.* 1985). Three pairs of field coils were rigidly attached to the superstructure and moved with the animal, so they generated three fields orthogonal to each other and aligned with the X (naso-occipital), Y (inter-aural), and Z (supero-inferior) head coordinate axes. The X, Y, and Z fields oscillated at 100 kHz, 50 kHz, and 75 kHz respectively. The three frequency components induced across each scleral coil were demodulated (Remmel, 1984) to produce three voltages proportional to the angles between the coil and each magnetic field. These were analyzed using 3D rotational kinematic methods detailed by Straumann *et al.* (1995). All signals transducing motion of

the head or the eye were passed through eight-pole Butterworth anti-aliasing filters with a corner frequency of 100 Hz and then digitized at a sampling rate of 1 kHz. Coil misalignment was corrected using an algorithm that calculated the instantaneous rotation of the coil pair with reference to its orientation when the eye was in a reference position (Hepp, 1999). Angular rotations were expressed as rotation vectors with roll, pitch and yaw coordinates, and angular velocity vectors of eye with respect to head were calculated from rotation vectors (Haslwanter 1995; Migliaccio and Todd 1999). Angular position resolution of the coil system was 0.2° (tested over the angular range of ±25° combined yaw, pitch, and roll positions), and peak angular velocity noise was approximately 2.5°/s.

Stimulation was performed with the head stationary and the animal in complete darkness, to ensure that observed eye movements were due solely to prosthetic stimulation. We used Johns Hopkins MVP2 prosthesis (Chiang *et al.* 2010) to deliver symmetric biphasic, charge balanced, 200 μs/phase and 100–200 μA/phase pulse trains via three ampullary electrodes with respect to a return electrode in the common crus. Each biphasic pulse comprised three fixed-duration intervals: a constant-current cathodic phase (during which the active electrode near the target nerve was cathodic and a reference electrode was anodic), a 25 μs zero-current interphase gap (or *intra*pulse interval), and a charge-balancing constant-current anodic phase during which the direction of current flow was reversed. Instantaneous pulse rate was defined as the reciprocal of the time from onset of one cathodic phase to the onset of the next. Pulses were presented concurrently but asynchronously, with only one electrode pair active at any given moment. Pulse rates were modulated to encode gyro signal inputs using a scheme described in detail elsewhere (Della Santina *et al,* 2007; Chiang *et al.,* 2010). In brief, the baseline stimulation rate on each channel was 94 pulses/sec. The MVP2's microcontroller was programmed so that its usual analog input ports for gyro signals that would normally encode head rotation about each SCC axis connected instead to analog signals controlled by the experimental apparatus, which could provide analog waveforms emulating head angular velocity about each axis by individually modulating each analog input. The operating curve mapping effective head velocity to pulse rate was designed to emulate normal rhesus vestibular afferent rate data reported by Sadeghi *et al.* (2007); it comprised a sigmoidal relationship with 47, 94 and 222 pulses/sec corresponding to -100, 0 and 100°/sec, respectively, where positive values indicate head rotations excitatory for the implanted labyrinth.

3 RESULTS

3.1 Confirmation of electrode location and function

Four rhesus monkeys underwent electrode implantation surgery, always in the left ear. Post-implantation computed tomography (CT) scans confirmed intralabyrinthine positioning of the prosthesis electrodes in each case (Figure 1). Eye movement responses to prosthetic stimulation delivered via each electrode were primarily about the axis of the corresponding semicircular canal (Figure 2), confirming proper location and function of the implant. For example, when the ampullary nerve of the left horizontal canal (LH) was stimulated, the eye responded by moving primarily about the axis of the LH canal. Appropriately directed eye responses were also observed when the left anterior (LA) and left posterior (LP) canal were stimulated, indicating that activity on each of the ampullary branches of the vestibular nerve could be semiselectively modulated by prosthetic stimuli. Response components about the axes of nontarget canals (e.g., the relatively small sinusoidal responses about the LA and LP canal axes during LH electrode stimulation in Figure 2, column 1) were consistent with excitation due to spread of stimulus current beyond the target ampullary nerve, but could also be attributed to small variations in labyrinth orientation with respect to the rest of the skull, as has been observed both in rhesus monkeys (Blanks *et al.* 1985) and humans (Della Santina *et al.* 2005). All four monkeys had similar responses to electrical stimulation.

3.2 Effect of vestibular prosthesis electrode implantation on ABR thresholds

To generate a set of normative data for subsequent ABR measurements, we tested ABR thresholds in the 8 ears of the 4 normal rhesus monkeys before any surgical procedure (Figure 3A). The average ABR hearing threshold was 28.7±4.4 dB (mean±SD) for clicks, 27.5±2.6 for 1 kHz pure tone pips, 23.8±1.7 for 2 kHz and 26.3±3.7 for 4 kHz. ABR thresholds were similar to previously reported results for rhesus monkeys (Torre *et al.*, 2004).

Each of the four monkeys underwent electrode implantation surgery in the left ear. Figure 3B shows post-implantation ABR thresholds 4 weeks after surgery. For implanted ears, the average post-implantation ABR hearing threshold was 33.8±2.5 dB for clicks, 32.0±2.6 for 1 kHz tones, 32.5±5.1 for 2 kHz tones, and 35.0±2.9 for 4 kHz tones. The maximum change in ABR hearing threshold (post- minus pre-implantation) observed for any sound stimulus in any individual implanted ear was 10 dB. The average change in ABR hearing threshold was 6.3±2.4 dB for clicks, 6.2±4.8 dB for 1 kHz tones, 7.5±4.9 dB for 2 kHz tones, 8.5±4.8 dB for 4 kHz tones (1-tailed paired t tests: $p>0.05$ for all except $p=0.04$ for 4 kHz). Assuming the click ABR threshold mean and variance for 8 normal ears are accurate estimates of the true population distribution, and assuming equal variances for pre- and post-operative measurements, a paired t test comparing ears before and after surgery would have statistical power of 90% to detect a true threshold increase of 10 dB.

Changes in ABR thresholds for the nonimplanted (right) ear provide an estimate of test-retest variation independent of electrode implantation. The change in ABR hearing threshold (post- minus pre-implantation) for nonimplanted (right) ears was 3.5±2.2 dB for clicks, 1.3±1.5 dB for 1 kHz tones, 5.0±2.8 dB for 2 kHz tones, and 5.0±2.5 dB for 4 kHz tones ($p>0.05$ for every case). This similar to the variability reported by Torre et al. (2004) for normal rhesus monkeys. The average post-operative interaural ABR threshold difference (left minus right) of all operated animals was 2.7±1.8 dB for clicks, 4.4±1.3 dB for 1 kHz tones, 4.4±1.5 dB for 2 kHz tones, and 7.3±1.3 dB for 4 kHz tones ($p>0.05$ for all except $p=0.007$ for 4 kHz).

In summary, the changes observed in ABR thresholds of implanted and nonimplanted ears from before to after surgery suggest that implantation of vestibular prosthesis electrodes causes some hearing loss, but that loss is likely to be less than 10 dB.

3.3 Effect of vestibular prosthesis electrode implantation on DPOAE thresholds

To generate a set of normative data for subsequent DPOAE measurements, we tested DPOAE levels in the 8 ears of the same 4 normal rhesus monkeys used for normative ABR testing. The mean DPOAE level was 3.8±1.0 dB for 1 kHz, 10.7±2.1 dB for 2 kHz, 12.2±2.4 dB for 3 kHz, and 9.1±1.7 dB for 4 kHz (Figure 4A). These DPOAE levels were within the range previously reported by other groups for the same species (Lasky *et al.*, 1995; Martin *et al.*, 1988; Park *et al.*, 1995).

Consistent with ABR results, comparison of DPOAE levels for left (implant-side) ears before and after surgery revealed a decrease of 2–14 dB in DPOAE level due to implantation (Figure 4B), but the only statistically significant decrease of DPOAE level occurred at 3 kHz ($p<0.05$ in a 1-tailed t test with paired samples, $n=4$). Using the 2 kHz DPOAE levels of normal and implanted ears as estimates of the true population distributions, a paired t test comparing implanted ears before and after surgery would have statistical power of 0.8 to detect a true threshold increase of 5 dB.

Figure 4B also compares post-operative DPOAE levels between implanted (left) ears and unimplanted (right) ears. The mean DPOAE absolute level difference (right/nonimplanted

minus left/implanted) for all operated animals was 3.8±2.4 dB for 1 kHz, 6.1±2.3 dB for 2 kHz tones, 4.1±1.8 dB for 3 kHz tones, 0.2±0.2 dB for 4 kHz tones (for each case, $p>0.05$ in a 1-tailed t test with paired samples, n =4). Similarly, Figure 5B reveals that mean distortion product / noise floor (DP/NF) ratios at 1, 2, 3 and 4 kHz in implanted ears were lower than in nonimplanted ears (by 2.6±1.2, 5.5±3.2, 4.1±2.7 and 7.8±4.5, respectively), but that difference was not statistically significant despite statistical power of 0.8 to detect a true difference of 10 dB.

In summary, we did not observe a statistically significant change in absolute DPOAE levels or DP/NF ratios attributable to implantation of vestibular prosthesis electrodes. Due to sample size limitations, we cannot exclude the possibility that a true difference <10 dB exists, and the fact that all changes in mean levels were in the same direction suggests that one does. However, our data do indicate that if a larger sample size ultimately confirms a true mean hearing change due to implantation, then that change is unlikely to exceed 10 dB.

3.4 Changes in hearing during electrical stimulation via a multichannel vestibular prosthesis

To investigate whether cochlear hair cell or auditory nerve function is compromised by prosthetic electrical stimulation of the vestibular nerve independent of surgical trauma due to electrode insertion, we measured ABR thresholds and DPOAE levels both prior to and during prosthetic vestibular nerve stimulation. As illustrated in Figure 3C, ABR thresholds increased during prosthetic vestibular stimulation relative to their post-implantation, non-stimulation baseline by 0.4 to 5.1 dB; however the difference was not significant (paired, two-tailed t test: $p>0.05$) at any tested frequency.

As shown in Figures 4C and 5C, DPOAE levels and DP/NF ratios decreased during prosthetic stimulation, suggesting some interference with cochlear function; however, the decrease of DP level was small enough (range over all ears and frequencies tested: 2–14 dB) that DP remained present above the noise floor at every frequency. The average interaural DPOAE level difference after implantation was 1.6±0.3 dB, 3.3±0.5 dB, 6.9±1.2 dB and 0.8±0.2 dB, in response to 1k, 2k, 3k, and 4k Hz stimuli, respectively. The average interaural DP-NF ratio difference (right minus left, ±SD) between contralateral and ipsilateral ears during prosthetic stimulation was 2.2±0.24, 2.245±0.35, 7.8±0.75, and 6.1±0.63 in response to 1k, 2k, 3k, and 4k Hz pure tone stimuli, respectively. There is no significant difference between these two sets of data ($p>0.05$, paired t test).

4 DISCUSSION

Currently, no adequate treatment exists for individuals suffering from chronic symptoms of profound bilateral loss of vestibular sensation unresponsive to vestibular rehabilitation exercises. A multichannel vestibular prosthesis that modulates electrical stimulation of the ampullary nerves based on measured head motion may offer a useful solution, but the risk of hearing loss or interference is an important consideration. Electrode implantation into the SCCs could compromise hearing through eliciting scar formation in the middle or inner ear or disruption of the endocochlear potential. Indeed, a prior study of vestibular electrode implantation in rodents revealed a large change of hearing (31–51 dB) in 4 of 6 implanted ears, while 2 of 6 retained nearly normal hearing (Tang *et al.*, 2009). In contrast, we found in rhesus monkeys that although implantation can cause a measurable loss of hearing (i.e., elevation of ABR thresholds and decrease in both DPOAE amplitudes and DP/NF ratios); this loss is more modest than the prior findings in rodents suggested.

There are at least two possible reasons that rhesus monkeys in the present study suffered less hearing loss than did rodents in the study by Tang *et al.* First, the electrodes used by Tang, *et*

al., were individual wires that required significant manipulation to position appropriately, while the electrode arrays used in the present study were prefabricated and embedded within silicone carriers predesigned to self-orient within the ampullae. Excessive manipulation during chinchilla implantations could have incurred a higher risk of inner ear injury. Second, electrode implantation in rhesus monkeys can be performed via a transmastoid approach that allows isolation and preservation of middle ear structures, whereas middle ear bones in the chinchilla are closer to the implantation site and thus more likely to be impacted by scar formation or overflow of the cement Tang, *et al.*, used to stabilize electrodes. Since only air conducted stimuli were used in the chinchilla study, Tang, *et al.* noted that conductive hearing loss could have contributed to the hearing loss they reported. In the present study, persistence of robust DPOAE responses indicates that little or no conductive hearing loss occurred in rhesus monkeys.

Considering that humans have inner ear morphology and size closer to that of rhesus monkeys than rodents, and noting that the electrode arrays and implantation techniques used with humans will likely be closer to those employed in the present study than those employed by Tang, *et al.* in rodents, it is likely that human vestibular implant recipients will experience a risk of hearing loss similar to the more modest loss we observed in monkeys.

In addition to the risks of surgery, vestibular electrode activation could interfere with normal cochlear nerve activity due to current spread beyond the target ampullary nerves. Although attempts have been made to characterize patterns of current spread in the implanted labyrinth (Hayden *et al.* 2008), the extent of this effect on cochlear function and cochlear nerve activity were previously unknown. In the present study, we found that activation of a multichannel vestibular prosthesis caused a 0–5 dB elevation in ABR thresholds and 2–14 dB decrease in DPOAE amplitudes. Although we did not attempt to quantify animals' subjective percepts of sound or tinnitus, none of the animals tested exhibited signs of discomfort or annoyance during baseline prosthetic stimulation. It is possible that the DPOAE changes we observed were due in part to a conductive loss caused by electrically-evoked activation of the stapedius; however, we observed no signs of facial musculature contraction at the electrical stimulus intensities we employed during hearing assessments.

In summary, we found that implantation of electrodes for use with a multichannel vestibular prosthesis caused up to 14 dB of hearing loss (by ABR, DPOAE, and DP/NF measurements) compared to control ears in rhesus monkeys. The degree of loss was not significant in this cohort of 4 animals, for which our assays were adequately powered to detect a true change of ≥10 dB in ABR threshold. Delivery of prosthetic electrical stimulation further reduced hearing by 0.4–7.8 dB, suggesting that current spread to cochlear hair cells and/or the cochlear nerve may cause some spurious activity that might be perceived as sound by an individual using a vestibular prosthesis. For the combination of implantation and prosthesis activation, the maximum hearing threshold change from baseline that we observed (across all animals and all sound stimuli employed) was 12.1 dB, while the minimum was 4.2 dB.

Postmortem histopathologic studies of temporal bones donated by individuals with cochlear implants have demonstrated significant damage to the inner ear structures, including fibrosis in the vestibule, collapse of the saccule, decrease in ganglion cells, and formation of hydrops in the inner ear (Tien *et al.*, 2002; Handzel *et al.*, 2006). We expect that implantation of vestibular prosthesis electrodes could ultimately engender similar histologic changes, but histologic examination of the animals implanted for this study must await completion of multiple long-term behavioral tests.

Research Highlights

- Multichannel vestibular prosthesis stimuli can restore the 3D vestibulo-ocular reflex
- Hearing is preserved within ~10 dB after vestibular prosthesis electrode implantation
- Hearing is preserved within ~14 dB during electrical stimulation of vestibular nerve

Acknowledgments

This research was supported by unrestricted grants from the United States National Institute on Deafness and Other Communication Disorders, grants R01DC9255 and R01DC2390. We thank Lani Swarthout for assistance with ABR measurements. DPOAE were collected with aid from Colleen Ryan-Bane and Alicia White.

References

Blanks RH, Curthoys IS, Bennett ML, Markham CH. Planar relationships of the semicircular canals in rhesus and squirrel monkeys. Brain Res. 1985; 340(2):315–324. [PubMed: 3896405]

Chiang B, Fridman GY, Dai C, Della Santina CC. Design and performance of a multichannel vestibular prosthesis that restores semicircular canal sensation in rhesus monkey. IEEE Trans Neural Syst Rehab Eng. 2010 (accepted pending minor revisions, Oct 2010).

Davidovics NS, Fridman GY, Chiang B, Della Santina CC. Effects of biphasic current pulse frequency, amplitude, duration and interphase gap on eye movement responses to prosthetic electrical stimulation of the vestibular nerve. IEEE Trans Neural Syst Rehab Eng. 2010 Sep 2. [Epub ahead of print] PMID: 20813652.

Della Santina CC, Potyagaylo V, Migliaccio AA, Minor LB, Carey JP. Orientation of human semicircular canals measured by three-dimensional multiplanar CT reconstruction. JARO. 2005; 6(3):191–206. [PubMed: 16088383]

Della Santina CC, Migliaccio AA, Hayden R, Melvin TA, Fridman GY, Chiang B, Davidovics NS, Dai C, Carey JP, Minor LB, Anderson ICW, Park H, Lyford-Pike S, Tang S. Current and Future Management of Bilateral Loss of Vestibular Sensation – An update on the Johns Hopkins Multichannel Vestibular Prosthesis Project. Cochlear Implants International. 2010; 11(s2):2–11.

Della Santina CC, Migliaccio AA, Patel AH. A multichannel semicircular canal neural prosthesis using electrical stimulation to restore 3-D vestibular sensation. IEEE Trans Biomed Eng. 2007; 54:1016–1030. [PubMed: 17554821]

Epley JM. Singular neurectomy: hypotympanotomy approach. Otolaryngol Head Neck Surg. 1980; 88:304–309. [PubMed: 7402672]

Gacek RR, Gacek MR. Results of singular neurectomy in the posterior ampullary recess. ORL J Otorhinolaryngol Relal Spec. 2002; 64:397–402.

Gong W, Merfeld DM. Prototype neural semicircular canal prosthesis using patterned electrical stimulation. Ann Biomed Eng. 2000; 28:572–581. [PubMed: 10925955]

Gong W, Merfeld DM. System design and performance of a unilateral horizontal semicircular canal prosthesis. IEEE Trans Biomed Eng. 2002; 49:175–181. [PubMed: 12066886]

Fridman GY, Davidovics NS, Dai C, Migliaccio AA, Della Santina CC. Vestibulo-Ocular reflex responses to a multichannel vestibular prosthesis incorporating a 3D coordinate transformation for correction of misalignment. JARO. 2010; 11(3):367–381. [PubMed: 20177732]

Handzel O, Burgess BJ, Nadol JB Jr. Histopathology of the peripheral vestibular system after cochlear implantation in the human. Otol Neurotol. 2006; 27:57–64. [PubMed: 16371848]

Haslwanter T. Mathematics of three-dimensional eye rotations. Vision Res. 1995; 35:1727–1739. [PubMed: 7660581]

Hayden, RP.; Mori, S.; Della Santina, CC. An electroanatomical/neuromorphic model to guide electrode design for a multichannel vestibular prosthesis. Abstr 792. Assoc for Research in Otolaryngology Ann Mtg; Phoenix: 2008.

Hepp K. On Listing's law. Commun Math Phys. 1990; 132:285–295.

Lasker DM, Hullar TE, Minor LB. Horizontal vestibuloocular reflex evoked by high-acceleration rotations in the squirrel monkey. III. Responses after labyrinthectomy. J Neurophysiol. 2000; 83:2482–2496. [PubMed: 10805650]

Lasky RE, Snodgrass EB, Laughlin NK, Hecox KE. Distortion product otoacoustic emissions in Macaca mulatta and humans. Hear Res. 1995; 89:35–51. [PubMed: 8600131]

Martin GK, Lonsbury-Martin BL, Probst R, Coats AC. Spontaneous otoacoustic emissions in a nonhuman primate. I. Basic features and relations to other emissions. Hear Res. 1988; 33:49–68. [PubMed: 3372370]

Migliaccio AA, Schubert MC, Jiradejvong P, Lasker DM, Clendaniel RA, Minor LB. The three-dimensional vestibulo-ocular reflex evoked by high-acceleration rotations in the squirrel monkey. Exp Brain Res. 2004; 159:433–446. [PubMed: 15349709]

Migliaccio AA, Todd MJ. Real-time rotation vectors. Australas Phys Eng Sci Med. 1999; 22:73–80. [PubMed: 10474978]

Minor LB, Lasker DM, Backous DD, Hullar TE. Horizontal vestibuloocular reflex evoked by high-acceleration rotations in the squirrel monkey. I. Normal responses. J Neurophysiol. 1999; 82:1254–1270. [PubMed: 10482745]

Minor LB, Goldberg JM. Vestibular-nerve inputs to the vestibulo-ocular reflex: A functional-ablation study in the squirrel monkey. The Journal of Neuroscience. 1991; 11:1636–1648. [PubMed: 2045879]

Paige GD, Tomko DL. Eye movement responses to linear head motion in the squirrel monkey. I. Basic characteristics. J Neurophysiol. 1991; 65(5):1170–1182. [PubMed: 1869911]

Park JY, Clark WW, Coticchia JM, Esselman GH, Fredrickson JM. Distortion product otoacoustic emissions in rhesus (Macaca mulatta) monkey ears: normative findings. Hear Res. 1995; 86:147–162. [PubMed: 8567411]

Remmel RS. An inexpensive eye movement monitor using the scleral search coil technique. IEEE Trans Biomed Eng. 1984; 31(4):388–390. [PubMed: 6745975]

Sadeghi SG, Minor LB, Cullen KE. Response of vestibular-nerve afferents to active and passive rotations under normal conditions and after unilateral labyrinthectomy. J Neurophysiol. 2007; 97(2):1503–1514. [PubMed: 17122313]

Straumann D, Zee DS, Solomon D, Lasker AG, Roberts DC. Transient torsion during and after saccades. Vis Res. 1995; 35:3321–3334. [PubMed: 8560803]

Tang S, Melvin TAN, Della Santina CC. Effects of semicircular canal electrode implantation on hearing in chinchillas. Acta Oto-Laryngologica. 2009; 129:481–486. [PubMed: 18615331]

Tien HC, Linthicum FH Jr. Histopathologic changes in the vestibule after cochlear implantation. Otolaryngol Head Neck Surg. 2002; 127:260–264. [PubMed: 12402002]

Torre P III, Mattison JA, Fowler CG, Lane MA, Roth GS, Ingram DK. Assessment of auditory function in rhesus monkeys (Macaca mulatta): effects of age and calorie restriction. Neurobiol Aging. 2004; 25(7):945–954. [PubMed: 15212848]

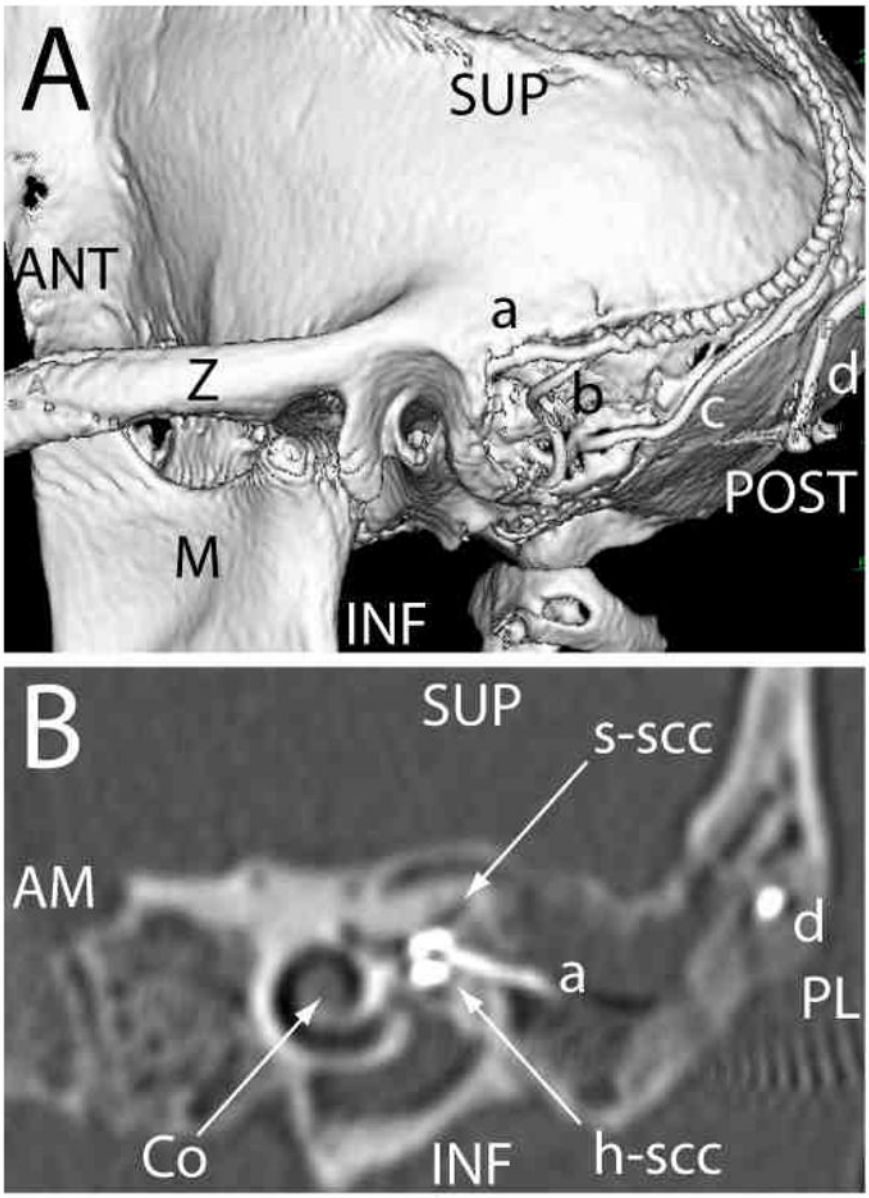

Figure 1. 3D computed tomography [CT] reconstructions of electrode array placement

(A) Posterolateral view of 3D CT surface reconstruction showing electrode array leads implanted in the left labyrinth of a rhesus monkey via the mastoid cavity. a: lead to anterior and horizontal ampullae; b: lead to posterior ampulla; c: common crus reference electrode; d: neck reference electrode; M: mandibular ramus; Z: zygomatic arch; ANT, POST, SUP, INF: anterior, posterior, superior, inferior. **(B)** Oblique CT cut through the plane of the basal turn of the cochlea [Co], showing bifurcated electrode array [a] entering the ampullae of the superior [s-scc] and horizontal [h-scc] semicircular canals. Part of the neck reference electrode [d] is also visible, but the posterior scc electrode array is not included in this section. AM, PL: anteriomedial, posterolateral.

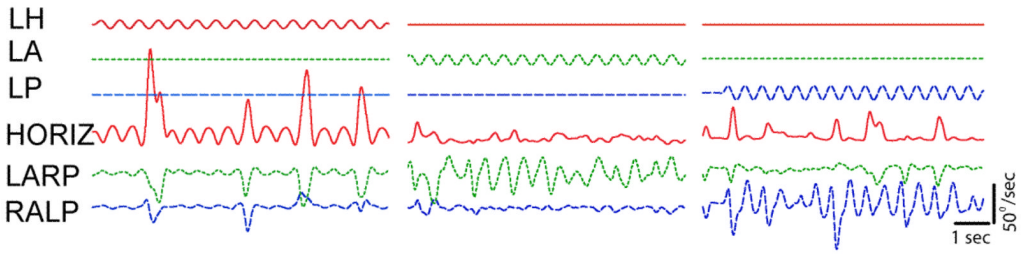

Figure 2. Eye movement responses

to pulse rate modulated, biphasic constant current pulses delivered via bipolar prosthesis electrodes implanted in the left labyrinth of a stationary alert rhesus monkey tested in darkness. Upper traces show stimulus waveforms modulating pulse rates on electrodes in the left horizontal (LH), left anterior (LA) and left posterior (LP) semicircular canal ampullary nerves. In each case, modulation frequency is 2 Hz, baseline pulse rate is 94 pulses/sec, modulation range is 48–222 pulses/sec, and the modulating waveforms shown were passed to the microprocessor of the prosthesis in place of actual gyro signals to emulate sinusoidally varying head velocity about each semicircular canal axis in an animal whose head remained still. Lower traces show eye movements about the mean horizontal (HORIZ), left-anterior/right-posterior (LARP), and right-anterior/left-posterior (RALP) axes of the head, which approximately align with the corresponding semicircular canals. Blinks and/or voluntary saccades are also evident as departures from the generally sinusoidal responses to prosthetic stimuli.

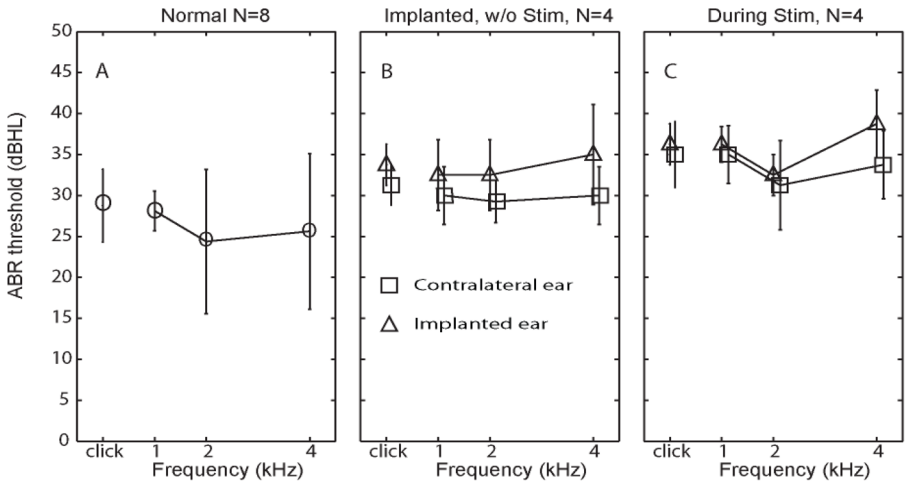

Figure 3. ABR thresholds in response to clicks and tone pips

(A) ABR thresholds [mean±SD] in response to clicks and pure tone pips at 1, 2 and 4 Hz, measured from eight normal ears in four rhesus monkeys. **(B)** ABR thresholds measured from implanted left ears (triangles) and nonimplanted right ears (squares) 4 weeks after surgery in four monkeys, prior to prosthesis activation. **(C)** ABR thresholds measured during prosthetic vestibular stimulation of the implanted ear (modulating over the range 48–222 pulses/sec).

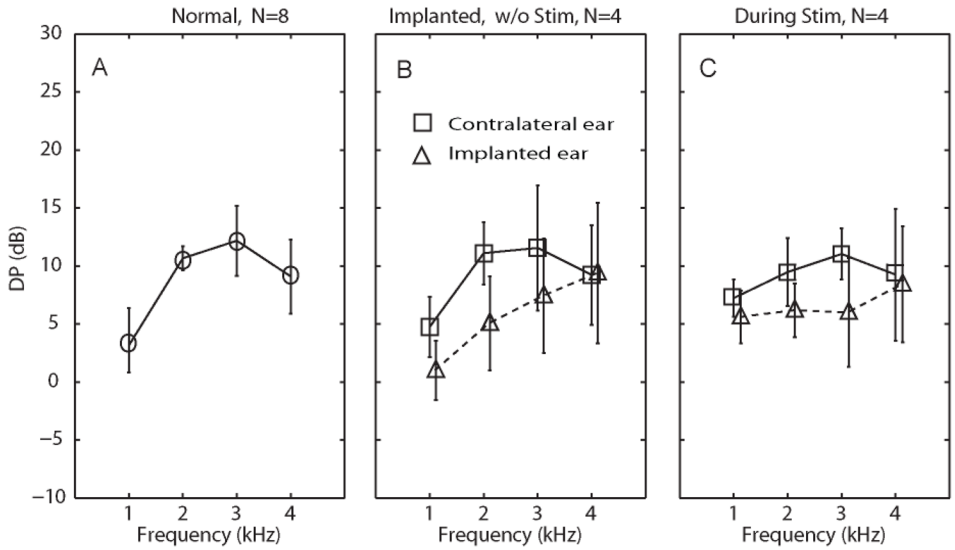

Figure 4. Absolute distortion product otoacoustic emission [DPOAE] response amplitudes

(A) DPOAE levels [mean±SD] in response to clicks and pure tone pips at 1, 2 and 4 Hz, measured from eight normal ears in four rhesus monkeys. **(B)** DPOAE levels measured from implanted ears (triangles) and contralateral ears (squares) 4 weeks after surgery in four monkeys, prior to prosthesis activation. **(C)** DPOAE levels measured during prosthetic vestibular stimulation of the implanted ear (modulating over the range 48–222 pps). In panels B and C, triangles represent left (implanted) ear and squares represent right (control) ear.

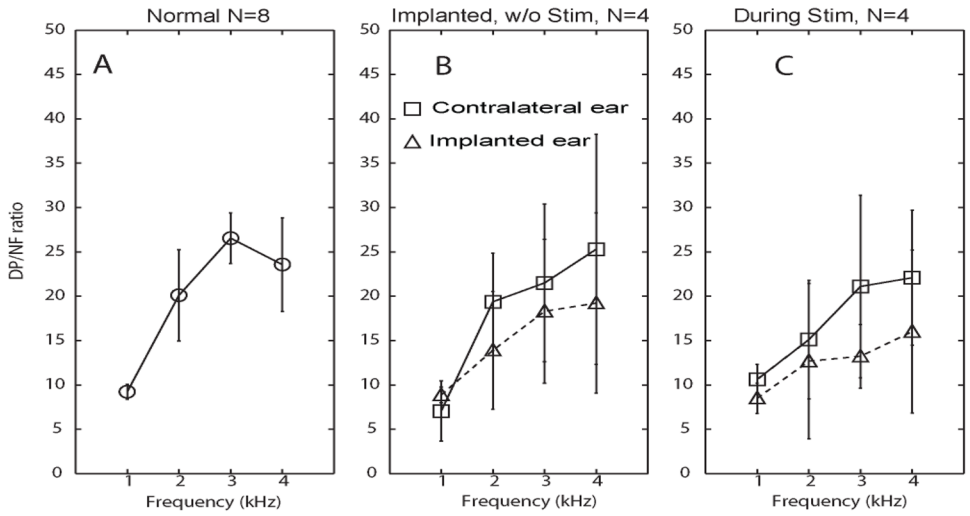

Figure 5. Distortion product vs. noise floor [DP/NF] ratios

(A) DP/NF ratio [mean±SD] in response to clicks and pure tone pips at 1, 2 and 4 Hz, measured from eight normal ears in four rhesus monkeys. **(B)** DP/NF ratio measured from implanted ears (triangles) and contralateral ears (squares) 4 weeks after surgery in four monkeys, prior to prosthesis activation. **(C)** DP/NF ratio measured during prosthetic vestibular stimulation of the implanted ear (modulating over the range 48–222 pps). In panels B and C, triangles represent left (implanted) ear and squares represent right (control) ear.